HIGH CHOLESTEROL LEVELS PROMOTE TNF-α-DEPENDENT NECROPTOSIS IN ALZHEIMER'S DISEASE

Xenia Abadín, Marlene Zubillaga, Elia Ivars, Ramón Trullás, Andrea Stavoe, Anna Colell

INSTITUT D'INVESTIGACIONS BIOMÈDIQUES DE BARCELONA, IIBB-CSIC

INTRODUCTION

Alzheimer's disease (AD) is characterized by extensive neuronal loss, however, how neurons die in the central nervous system still remains unclear. A recent study offers compelling evidence of active necroptosis, a regulated inflammatory cell death, in post-mortem AD brains (**1**), but still, the events that trigger or regulate necroptosis in AD are not fully known. Autophagy has been shown to protect cells from necroptotic cell death and act as a negative regulator of necroptosis (2). Moreover, our previous studies indicate that intracellular cholesterol accumulation can disrupt autophagy function (3), a pathological hallmark in multiple age-related neurodegenerative diseases, including AD. This study aims to evaluate the relationship between high cholesterol levels, altered autophagy, and necroptosis in AD.

METHODS

- APP-PSEN1-SREBP2 transgenic mice were generated from crossbreeding of B6C3-Tg(APPswe, PSEN1dE9)85Dbo/J mice [express a chimeric mouse/human amyloid precursor protein (isoform 695) with the Swedish mutation (Mo/HuAPP695swe) and mutant human presenilin 1 (PSEN1dE9)] and B6; SJL-Tg(rPEPCKSREBF2)788Reh/J mice that overexpress the active form of the sterol regulatory element binding protein 2. These mice display increased total brain cholesterol levels and selective depletion of mitochondrial GSH levels (**4**).
- Embryonic cortical-hippocampal neurons were isolated from mice at gestational days 16-17 by trypsin digestion following a standard protocol (**5**). Dorsal Root Ganglia (DRG) isolation and primary cultures were performed as previously described (**6**).
- Cholesterol enrichment was assessed by incubating the cells with a soluble cholesterol/methyl-cyclodextrin complex (50 mg/ml) for 1 h, followed by 4 h of recovery. The necroptotic pathway was induced through treatment with TNFα (60 ng/ml), the pan-caspase inhibitors qVD-Oph (10 µM), and the SMAC mimetic LCL-161 (10 µM) at the indicated times.

RESULTS

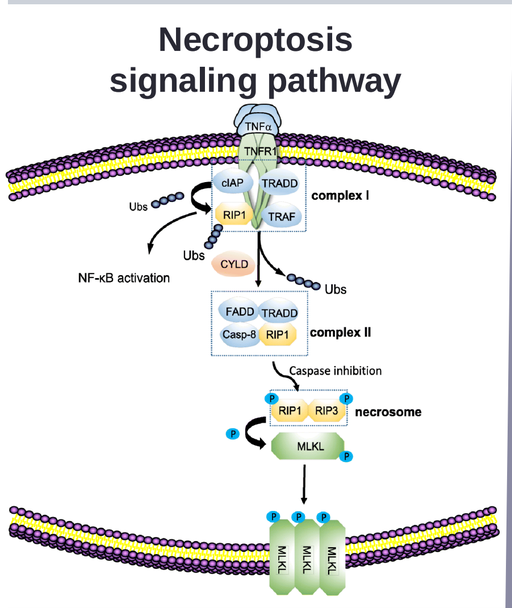

1

Cholesterol-enriched SH-SY5Y cells display increased cell death inhibited by RIPK1 and RIPK3 inhibitors. A) Representative confocal images showing dying cells (stained with 7-AAD) with intact nuclei when exposed to TNF plus LCL-161 and qVD-Oph for 48h. Scale bars, 10µm **B**) Representative confocal images showing the protective effect of necrostatin (RIPK1 inhibitor) and GSK'782 (RIPK3 inhibitor). n= 50-100. **p<0.01. Scale bars, 20µm

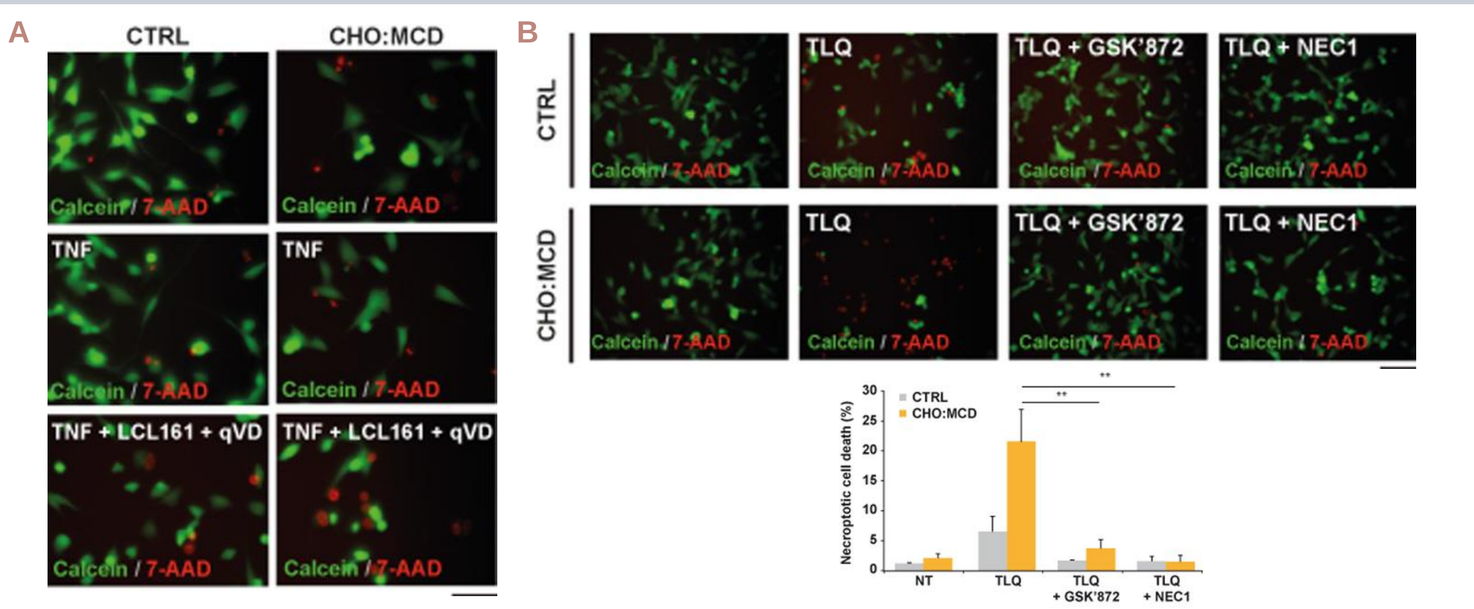

2

Enhanced necrosome assembly in 9 month-old APP-PSEN1-SREBP-2 mice. A) Sequential solubility analysis of RIPK1 and MLKL showed an increased presence of the necroptotic proteins in high insoluble fractions of brain lysates from APP-PSEN1-SREBF2 mice. F1: TBS soluble , F2: 1% Triton soluble, F3: 2% SDS soluble, F4: 8M urea soluble. **B)** Western blot analysis of RIPK3 and MLKL brain lysates of WT and transgenic mice, showing increased presence in urea soluble fraction. **C**) Urea-soluble fractions of WT and transgenic mice showing an increased presence of pRIPK3 in APP-PSEN1-SREBF2 mice. D) Representative immunoblot of p-MLKL in WT and transgenic mice showing increased presence of the protein in APP-PSEN1-SREBF2 lysates.

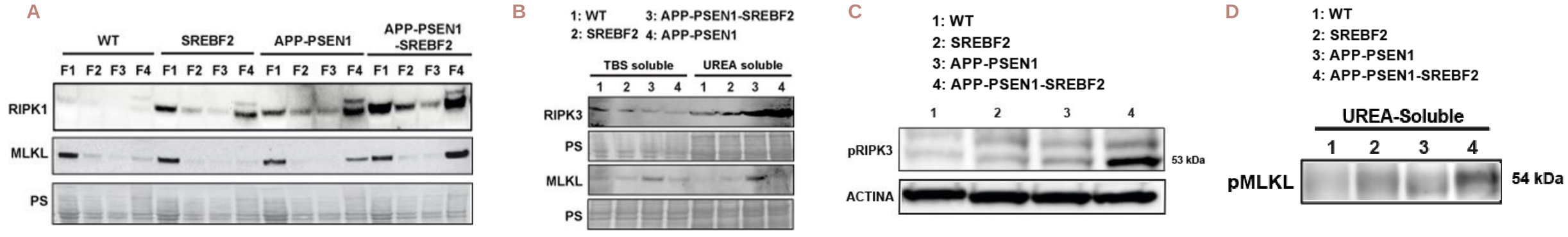

3

Higher levels of phospho-RIPK3 and phospho-MLKL in primary neurons derived from APP-PSEN1-SREBF2 mice. A) Representative immunoblots of pRIPK3 showing increased expression in APP-PSEN1-SREBF2 derived neurons compared to WT**. B)** Western blot analysis showing increased presence of p-MLKL in APP-PSEN1 and APP-PSEN1-SREBF2 primary neurons. **C)** Representative confocal images of primary neurons derived from WT and APP-PSEN1-SREBF2 mice immunostained with p-RIPK3 (green) and p-MLKL (red). Nuclei were counterstained with Hoechst (blue). Scale bar, 10 µm.

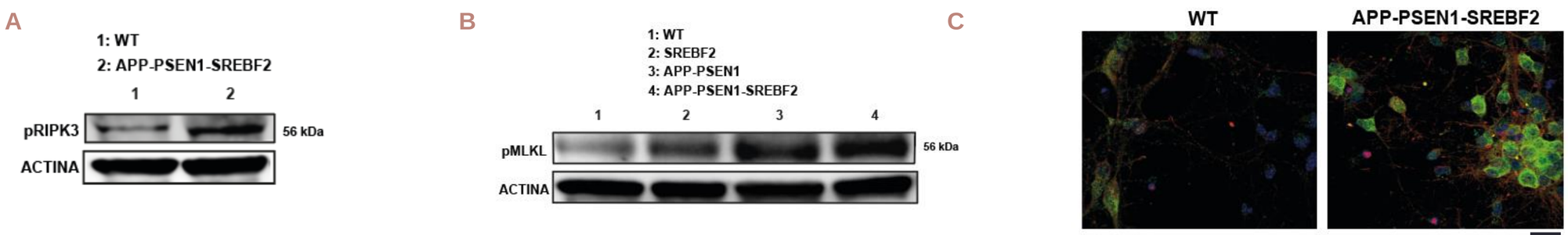

4

Phosphorylated RIPK3 and MLKL constitutively expressed in DRG from aged mice (15 months). A) Representative confocal images of young (3-month-old) and old (15-month-old) DRG neurons immunostained with p-RIPK3 (green) and p-MLKL (red). The nuclei are stained with Hoechst (blue). The plot represents p-RIPK3 and p-MLKL levels per cell, quantified as the CTCF of the green and red channels (n=12-16 non-overlapping images from different mice).
B) Representative confocal images of aged DRGs with Halo-WIPI2-S395A (light blue), co-immunostained with p-RIPK3 (green) and p-MLKL (red), showing that restoring autophagy with WIPI2 decreases the expression of necroptotic proteins. Scale bar, 10 µm.

CONCLUSIONS

The activation of the necroptotic pathway and inflammatory cell death in AD is favoured by increased intracellular cholesterol load and defective autophagy linked to aging.

Acknowledgements: This work was supported by grants from Ministerio de Ciencia y Innovación (RTI2018-095572-B-100 and PID2020-115091RB-100), AGAUR (SGR00490 and 2021FI_B00627)

REFERENCES

1. Caccamo A, et al. Necroptosis activation in Alzheimer's disease. Nat Neurosci. 2017; 20(9):1236-46.
2. Xu C, et al. TNF-α-dependent neuronal necroptosis regulated in Alzheimer's disease by coordination of RIPK1-p62 complex with autophagic UVRAG. Theranostics. 2021;11(19):9452.
3. Roca-Agujetas V, et al. Upregulation of brain cholesterol levels inhibits mitophagy in Alzheimer disease. Autophagy. 2021;17(6):1555–7.
4. Barbero Camps E, et al. APP/PS 1 mice overexpressing SREBP 2 exhibit combined A β accumulation and tau pathology underlying Alzheimer's disease. Hum Mol Genet 2013; 22 (17): 3460-76.
5. Kaech S, Banker G. Culturing hippocampal neurons. Nat Protoc. 2006; 1(5):2406-15.
6. Perlson E, Jeong GB, Ross JL, Dixit R, Wallace KE, Kalb RG, et al. A switch in retrograde signaling from survival to stress in rapid-onset neurodegeneration. J Neurosci. 2009;29(31):9903–17.